Biomaterials 31 (2010) 5678–5688

Contents lists available at ScienceDirect

Biomaterials

journal homepage: www.elsevier.com/locate/biomaterials

Pore size variable type I collagen gels and their interaction with glioma cells

Ya-li Yang [1], Stéphanie Motte, Laura J. Kaufman*

Department of Chemistry, Columbia University, New York, NY 10027, USA

ARTICLE INFO

Article history:
Received 19 January 2010
Accepted 16 March 2010
Available online 29 April 2010

Keywords:
Collagen
Hydrogel
Self-assembly
Elasticity
Cell morphology

ABSTRACT

Gelation temperatures from 22 °C to 37 °C were used to control the pore size of collagen matrices independent of collagen concentration. To limit cell exposure to temperatures lower than physiological temperature, the putative nucleation and growth mechanism of collagen was investigated to determine the time at which gel fibril and network structure becomes independent of temperature. It was found that the temperature dependent portion of collagen gelation ends close to the time at which fibrils first form a network spanning structure. These findings were then exploited to prepare cell-embedded gels nucleated at 22, 27, or 32 °C and then incubated at 37 °C. This achieves fibrillar and network structure characteristic of gels formed solely at the nucleation temperature. Proof of principle studies of glioma invasion in these gels suggested pore size is a key determinant of glioma invasive speed in collagen gels.

1. Introduction

Extracellular matrix (ECM), a complex mixture of biomacromolecules and water, regulates cell motility, proliferation, differentiation, and apoptosis through biochemical and biophysical cues [1–3]. To date, most *in vitro* studies investigating how ECM affects cell behavior have focused on how biochemical composition affects cellular response. More recently, the influences of physical properties of ECM and ECM approximations on cell behavior have garnered attention [3–12]. With notable exceptions [4,10,12], studies in this area have typically been performed on two-dimensional substrates, as decoupling biochemistry, topology, and mechanical properties in three-dimensional (3D) environments is especially challenging. Despite the challenges, to more fully understand the reciprocal interactions between cells and ECM, it is crucial to develop physiologically relevant 3D matrices in which biochemical and physical parameters of the environment can be independently tuned.

Collagen I is the most prevalent protein in ECM, and networks composed of this protein are commonly used in cell studies [7,13]. Such networks hold promise of significant tunability, as their structure and mechanical properties can be adjusted via changes in pH, ionic strength, and temperature during self-assembly [14–21]. However, the dimensions and organization of collagen fibrils can only be changed modestly within ranges of pH, ionic strength, and temperature consistent with cell viability. Here, we present a simple method that overcomes this limitation by exploiting the putative nucleation and growth mechanism of collagen self-assembly [22,23]. Specifically, we nucleated cell-free solutions and cell-embedded collagen suspensions at 22, 27, or 32 °C for a short time before incubating the systems at 37 °C for the later stages of collagen self-assembly. We then assessed network structural parameters and cell viability and proliferation in these gels. In particular, we studied high grade glioma cells, which have extraordinary ability to invade through the uniquely crowded environment of brain tissue [24–26]. Recent studies have suggested that this efficient invasion may be related to glioma cells' capacity to alter their size and squeeze through small pores [27,28]. Thus, we use our model system to preliminarily investigate glioma invasion as a function of collagen gel pore size, independent of protein concentration. More broadly, we suggest that the approach taken here, harnessing the nucleation and growth mechanism of collagen self-assembly, can be utilized to generate complementary sets of networks that allow assessment of the independent importance of biochemical, topological, and mechanical properties of 3D environments on cell behavior.

2. Materials and methods

2.1. Materials

High concentration type I collagen extracted via acid-solubilization of rat tail tendon was obtained from BD Biosciences. The solution was delivered at ~10 mg/ml in 0.01 M acetic acid, with exact concentration varying by lot. 10× Dulbecco's Modified Eagle Media (DMEM), bicarbonate (7.5%) and sterile NaOH (1 N) were purchased from Sigma Aldrich. Gibco HEPES buffer (1 M) and collagenase type I were obtained from Invitrogen.

* Corresponding author. Tel.: +1 212 854 9025.
E-mail address: kaufman@chem.columbia.edu (L.J. Kaufman).
[1] Present address: Department of Mechanical Engineering, University of California, Santa Barbara, Santa Barbara, CA 93106, USA.

0142-9612/$ – see front matter © 2010 Elsevier Ltd. All rights reserved.
doi:10.1016/j.biomaterials.2010.03.039

2.2. Cell lines and cell culture

C6 rat glioma cells and C6 cells labeled with green fluorescent protein (C6-GFP) were provided by Peter Canoll (Columbia University Medical Center, NY). Cells were cultured in DMEM supplemented with 10% heat-inactivated fetal bovine serum (FBS) and 1% antibiotic–antimycotic solution (containing 10 000 U/ml penicillin, 10 000 μg/ml streptomycin, and 25 μg/ml amphotericin B). Cells were maintained at 37 °C with 5% CO_2 and trypsinized and subcultured when ~80% confluent.

2.3. Preparation of glioma spheroids

Multicellular tumor spheroids (MTSs) of uniform size and shape were formed using a hanging drop procedure. Cells were cultured on 2D substrates, harvested, and re-suspended in culture medium at a concentration of 2.5×10^4 cells/ml. 20 μl cell suspension with ~500 cells was dropped on the inside cover of a 100 mm Petri dish, and the Petri dish was filled with 10 ml culture medium. The dish cover was inverted and incubated for 7 days. The drops were held in place by surface tension. Cells accumulated at the bottom of the droplet to form spheroids of ~400 μm diameter after 7 days.

2.4. Collagen gel preparation

Appropriate amounts of the ~10 mg/ml stock collagen solution, depending on the final concentration desired, were mixed at 4 °C with 10% (v/v of the final solution) 10× DMEM, 2.5% (v/v) HEPES buffer, 2.5% (v/v) sodium bicarbonate, and 1% (v/v) FBS. 0.5 N NaOH was added to adjust the pH to 7.4. Sterile water was added to reach the desired total volume. The solution was prepared and kept at 4 °C. Final ionic strength of gel solutions is $I \sim 0.13$. Gel matrices were formed by incubation at 22–37 °C.

2.5. Preparation of cell-embedded collagen gels

To prepare collagen gels loaded with dispersed cells for single cell imaging, cell suspension at a density of 5×10^5 cells/ml was mixed with a collagen solution at a ratio of 1:9 (v/v) at 4 °C. The mixture was then added to a chamber consisting of a 2 cm diameter plexiglass cylinder sealed on a coverslip pre-coated with a thin layer of collagen. A nylon mesh was added to the inner circumference of the sample cell cylinder to anchor the collagen gels. The suspension was then either incubated at 37 °C or first incubated in a temperature controlled environment at 22, 27, or 32 °C for 30 min before transfer to an incubator at 37 °C. After gelation was complete, fresh culture medium was added atop the gel and supplemented daily.

To prepare collagen gels loaded with a spheroid, a single spheroid was placed into a sample cell containing 400 μl of collagen solution on ice. The sample cell was then covered and incubated at 37 °C, or first incubated at 22, 27, or 32 °C for 30 min before transfer to an incubator at 37 °C. Spheroids were imaged and invasive distance (as depicted by the arrow in Fig. 7a) was measured 2, 24, 48, and 72 h after implantation. 100 μl of culture medium was added atop the gel at each of these intervals after imaging.

2.6. Cell viability measurements

To prepare collagen gels with dispersed cells for viability measurements, C6 cells at 2×10^6 cells/ml in culture medium were mixed with 1.0 mg/ml collagen solution at 1:9 (v/v) ratio in an ice bath. 0.5 ml of cell containing collagen suspension was added into wells of a 24-well plate and gelled at the chosen temperature(s). 100 μl of fresh culture medium was added on top of each gel after 1, 24, 48, and 72 h of incubation. After 24, 48, and 72 h of incubation, cell viability and proliferation were measured by a Trypan Blue exclusion assay and hemocytometer counting. 0.5 ml collagenase solution (1000 U/ml) was added to each well, mixed with the collagen gel, and incubated at 37 °C for 30–45 min until the collagen gel was completely digested. Cells were collected and re-suspended in 0.25 ml culture medium, mixed with 0.05 ml 0.4% Trypan Blue and allowed to stand ~3 min at room temperature. Non-viable cells stained blue and viable cells excluding the stain were counted using a hemocytometer. Viability measurements were done on 6 samples at each time point.

2.7. Rheology

Rheological experiments were conducted on cell-free collagen gels on an AR-2000 rheometer with built-in temperature and gap calibration (TA Instruments). A 1° acrylic cone geometry with a solvent trap was used. All experiments were conducted in oscillatory mode at a fixed frequency of 1 Hz with a controlled strain of 0.8%. In all cases, 1 ml of collagen solution was neutralized and then applied to the measuring stage at 4 °C. After applying the sample, a solvent trap was added, and the measurement began when the tool reached the desired temperature (37, 32, 27 or 22 °C). For two-stage two-temperature rheology studies, the first step was performed at 22 °C for a time t_1, and the second step was performed at 37 °C. The temperature equilibrated to 37 °C within one minute of the initiation of the change. The time-sweep measurement thus ran for a time, t_1, halted upon initiation of the temperature change, and resumed when the sample reached 37 °C, at $t_1 + \sim 1$ min. Storage modulus, G′ (Pa), and loss modulus, G″ (Pa), were monitored as the gel formed until plateau values were attained. The final moduli were determined by averaging the last 10 points in the plateau regions. All tests were repeated at least three times.

2.8. Microscopy and image analysis

Transmitted light images of cells and confocal reflectance microscopy (CRM) images of collagen were recorded (in some cases, simultaneously) on an inverted confocal laser scanning microscope (Olympus Fluoview 300/IX-71). An argon ion laser at 488 nm was used to illuminate the sample, and the transmitted and/or reflected light was detected with photomultiplier tube (PMT) detectors. Confocal fluorescence microscopy (CFM) images of C6-GFP cells were recorded using the same laser and detector as CRM.

Mesh size was determined for both cell-free and spheroid-embedded collagen gels. For spheroid-embedded gels, mesh size was determined both far from and adjacent to the spheroid two hours after implantation. In images adjacent to the spheroid, a small portion of the MTS was present in one corner of the images. The bright CRM artifact in the center of the image and, when present, the small area covered by the MTS were replaced by regions with collagen fibers from elsewhere in the image. The images were then thresholded, and a histogram of distances between above-threshold pixels was plotted. The characteristic mesh size ξ was extracted by fitting the distribution to the function $y = Ae^{(-x/\beta)}$, with x distance in microns and $\xi = 1/\beta$. Mean and standard deviation are reported. At least 3 images were evaluated for each type of gel discussed.

Fibril diameter was estimated in gels constructed at 37 °C from SEM measurements reported previously [21]. To estimate structural diameter in gels nucleated at 22 °C, the relationship $G' = c\xi^{-4.4}d^{5.6}$ is employed. Here, ξ is measured mesh size, G′ is measured stiffness, and d is an average structural diameter averaged over individual fibrils and fibril bundles. The proportionality constant, c, was obtained from a best fit line to the data for 37 °C gels used in this study. The relationship $G' = c\xi^{-4.4}d^{5.6}$ has been found to fit acid-solubilized collagen formed over a range of concentrations and temperatures previously [21,29].

3. Results

3.1. Temperature dependence of gelation

Gelation of 1.0 mg/ml collagen at different temperatures from 22 °C to 37 °C was studied by rheology, with the storage modulus (G′) and loss modulus (G″) measured as a function of time during the self-assembly process (Fig. 1a). Rheological measurements at 22 °C revealed sigmoidal curves for the development of G′ and G″: there was a lag phase in which G′ and G″ were small and did not change significantly followed by a growth phase in which both G′ and G″ increased rapidly until reaching plateau values. Increasing the gelation temperature sped up the gelation as indicated by the shortened lag phase and the more rapid appearance of the plateau. Gelation at 32 °C showed no lag phase, and gelation at 37 °C showed only the plateau region. The sigmoidal shape of the G′ and G″ curves for gelation at 22 °C was very similar to that we measured previously for pepsin-solubilized collagen at 32 °C and 37 °C [30]. Consistent with earlier studies, the presence of intact telopeptides in acid-solubilized collagen correlated with much faster self-assembly of the monomers than for pepsin-solubilized collagen lacking telopeptides gelled at the same temperature [23,31–34].

The build-up of storage modulus during gelation can be related to the evolution of collagen fibril and network structure as described previously [30,35,36]. An example of gelation of 1.0 mg/ml collagen solution at 22 °C recorded by time-lapse CRM is shown in Fig. 1b. Initially no structures were resolved, consistent with a solution of monomers. After 10 min, several short, homogeneously distributed structures were apparent, and motion of these structures relative to one another was observed. Between 10 and 20 min, growing structures started to interconnect, a necessary condition for formation of a stable network. We term the moment at which the structures stop moving relative to one another the arrest time, and for 1.0 mg/ml acid-solubilized collagen gelled at 22 °C, this time was 21 ± 2 min for the 4 collagen gels followed in this manner. We found here, consistent

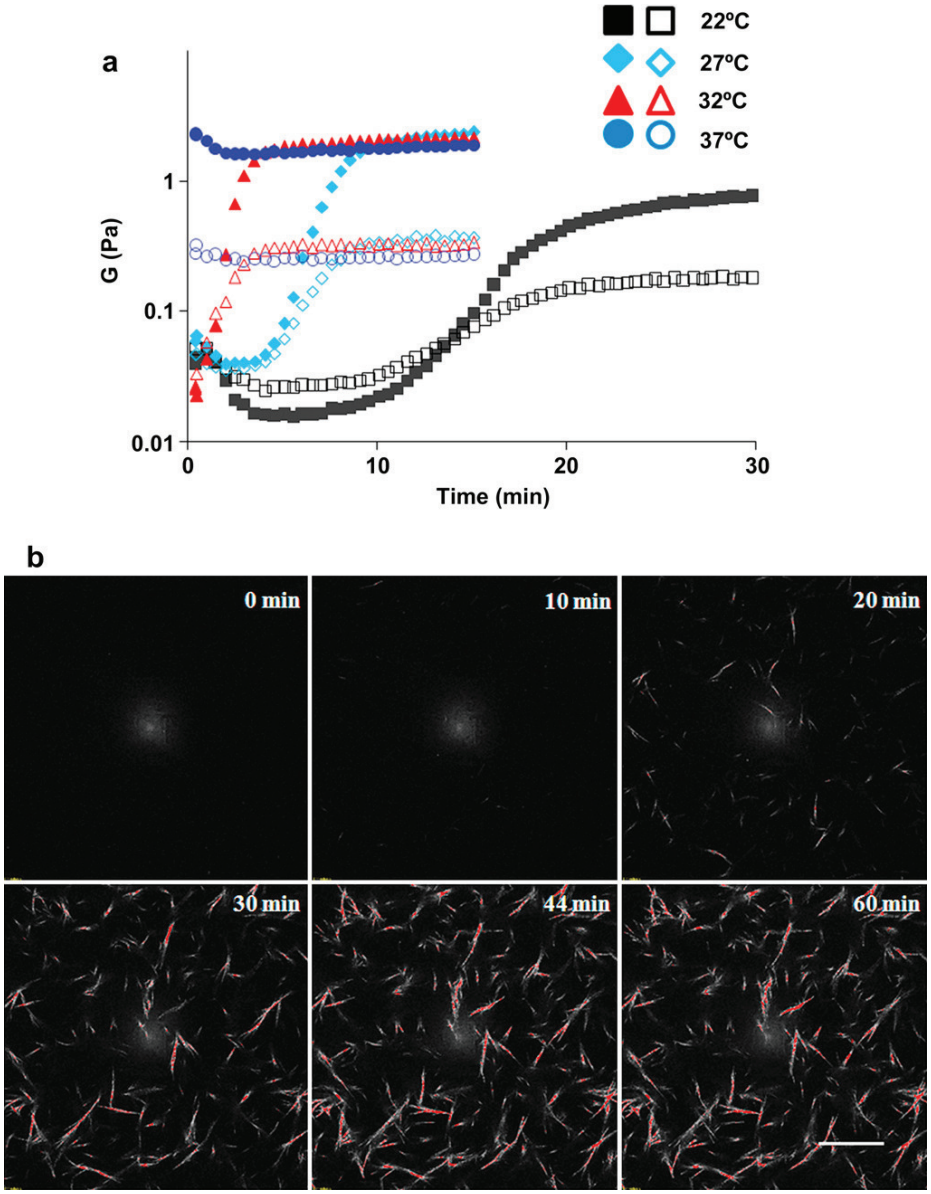

Fig. 1. Gelation of 1.0 mg/ml acid-solubilized collagen at 22 °C (black squares), 27 °C (cyan diamonds), 32 °C (red triangles), and 37 °C (blue circles). (a) Oscillatory time-sweep at various gelation temperatures. Closed symbols are storage modulus, G′, and open symbols are loss modulus, G″. (b) Time-lapse CRM during gelation at 22 °C. Arrest time occurred at ~20 min. Scale bar is 20 μm.

with our previous result, that arrest occurs in the presence of relatively few structures, and that the arrest time measured by CRM corresponds to the lag phase plus a substantial portion of the growth phase as measured by rheology [30]. Between 20 and 30 min, new structures continued to appear and structures present earlier lengthened and thickened even though storage and loss moduli were close to their equilibrium values by this point. This implies that changes to collagen fibers and the network after the arrest time do not contribute substantially to the development of the storage and loss moduli. Complete gelation of 1.0 mg/ml collagen at 22 °C occurred by 45 min, and we found no difference in CRM signal between 45 and 60 min. At all temperatures investigated, both CRM and rheology suggest that gelation was complete within 1 h.

3.2. Two-step, two-temperature gelation

It has been proposed that collagen self-assembly occurs in two distinct steps, a nucleation step and a growth phase [22]. The nucleation phase is expected to be temperature dependent and to set the number and diameter of collagen fibrils in a gel of given concentration [14,22,23,31]. To investigate whether this is the case and potentially define the duration of the temperature dependent phase in the collagen system used here, two-step two-temperature gelation experiments were performed. In these experiments, collagen solutions were incubated first at 22 °C (in a temperature controlled box) for a given amount of time and then transferred to a 37 °C environment (in an adjacent temperature controlled box) for the remainder of the gelation process. According to the

nucleation and growth hypothesis, if the time at 22 °C is longer than the nucleation time, the equilibrium properties of the gels should be identical to those of gels held at 22 °C for the entirety of the gelation process.

Two-step, two-temperature gelation was carried out on 1.0 mg/ml collagen: the collagen solution was kept at 22 °C for 0, 5, 10, 20, 30 or 45 min and then transferred to an incubator at 37 °C for 1 h (Fig. 2a). As the time held at 22 °C became longer, an increased number of thick fibers and fewer thin fibers were seen, and characteristic pore size increased. The most dramatic change in network structure was noted between the samples kept at 22 °C for 10 and 20 min. The two-stage gelation experiments suggested that the temperature dependent nucleation at 22 °C ended between 10 and 20 min. This was also the typical time scale for arrest as measured by CRM and corresponds to the lag phase and a proportion of the growth phase as measured by rheology as can be seen in Fig. 1a. We note that minor changes in fiber and network structure were observed for samples held at 22 °C for 20 and 30 min. Thus, growth during this period did not appear fully temperature independent. The minor differences in morphology between these gels may be related to mechanical disturbance of the gel during the transfer of the sample between temperature controlled environments, as it has been noted that mechanical agitation can dissolve small collagen aggregates, amounting to reverse nucleation [14]. No obvious difference in network structure was evident for systems held at 22 °C for 30 and 45 min. To quantify changes in network

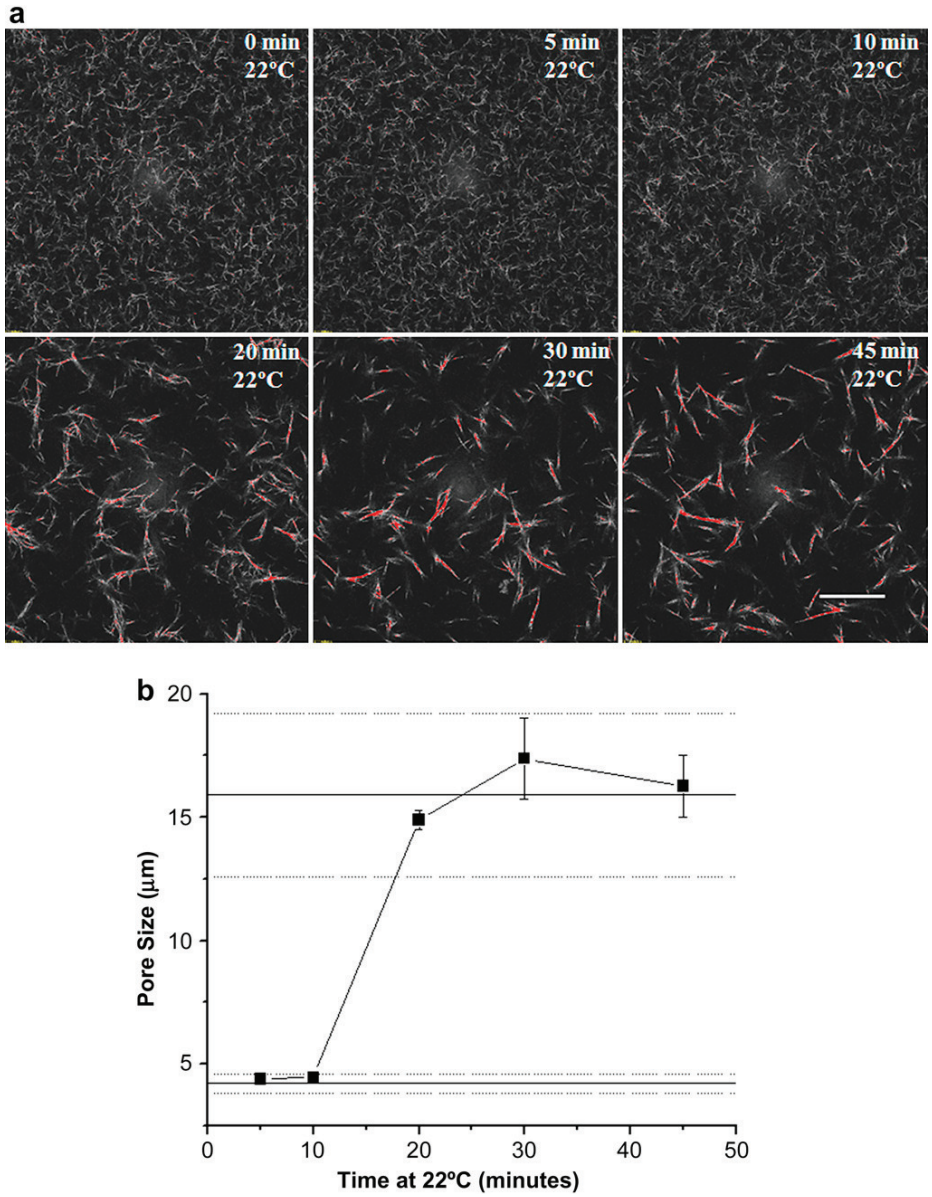

Fig. 2. (a) CRM images from two-stage two-temperature experiments to determine length of the temperature dependent portion of gelation of 1.0 mg/ml collagen at 22 °C. Collagen was incubated at 22 °C for the time period specified on the image and then incubated at 37 °C to complete gelation before imaging. Scale bar is 20 μm. (b) Pore size of gels held at 22 °C for a given amount of time. Solid lines indicate average pore size of 1.0 mg/ml gels constructed entirely at 37 °C (line at 4.4 μm) and those constructed entirely at 22 °C (line at 15.9 μm). Dotted lines indicate ± one standard deviation for the gels constructed at 37 and 22 °C.

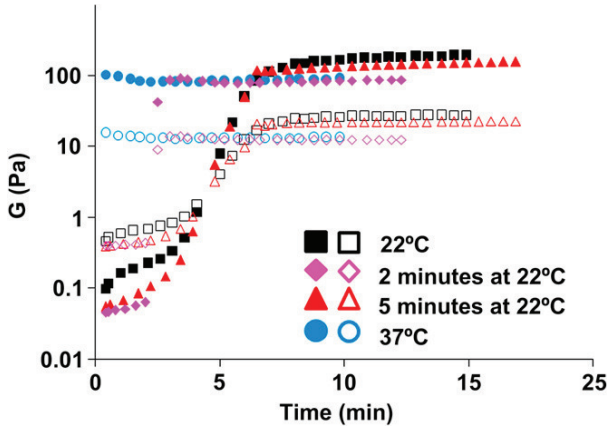

Fig. 3. Two-stage two-temperature experiment to determine the nucleation time of 4.0 mg/ml collagen at 22 °C by rheology. Collagen is gelled solely at 37 °C (blue circles) or at 22 °C (black squares). The lag time and the time of G′ (closed symbols) and G″ (open symbols) cross-over were found to be ~2 min and ~5 min, respectively. Collagen was then gelled first at 22 °C for 2 min (pink diamonds) or 5 min (red triangles) and then at 37 °C until plateau. There was a ~30-s lag while the temperature equilibrated to 37 °C, and the second stage started after this lag.

structure as a function of time at 22 °C, characteristic pore size in these gels was measured (Fig. 2b). Fig. 2b shows that pore size expected for collagen solutions gelled entirely at 22 °C was already established by 20 min even though, as revealed in Fig. 1b, few fibers were present in the system at that point.

We note that while the late stages of gelation were temperature independent with respect to final fiber and network structure, traditional rheological and microscopic definitions of nucleation occur earlier than the time point at which the temperature dependent portion of gelation was complete in our experiments. Indeed, for collagen of 1.0 mg/ml gelled at 22 °C, the lag phase as defined by rheology ended by 10 min. At this point there were very few fibrillar structures evident in the system. By 20 min, however, much of the growth phase as probed by rheology was complete. Although there were relatively few fibers in the system at that time, those present were sufficient to span the sample, causing a stabilization of the network that we have previously termed arrest [30]. As such, it appears that conditions required to set equilibrium gel structure extend somewhat beyond traditional definitions of nucleation, where only small aggregates that contribute little to storage modulus and are not reflective enough to be visualized via CRM would be present. This is further supported by additional tests of the two-step two-temperature gelation hypothesis performed with rheology. Here, collagen of 4.0 mg/ml rather than 1.0 mg/ml was used since difference in final storage modulus was expected to be clearer at relatively high collagen concentration [21]. Collagen at 4.0 mg/ml was first gelled at 22 °C and 37 °C. The lag time for 4.0 mg/ml collagen gelation at 22 °C was found to be ~2 min. The cross-over time, the time at which G′ becomes greater than G″, was ~5 min. This cross-over time has been shown to track but be

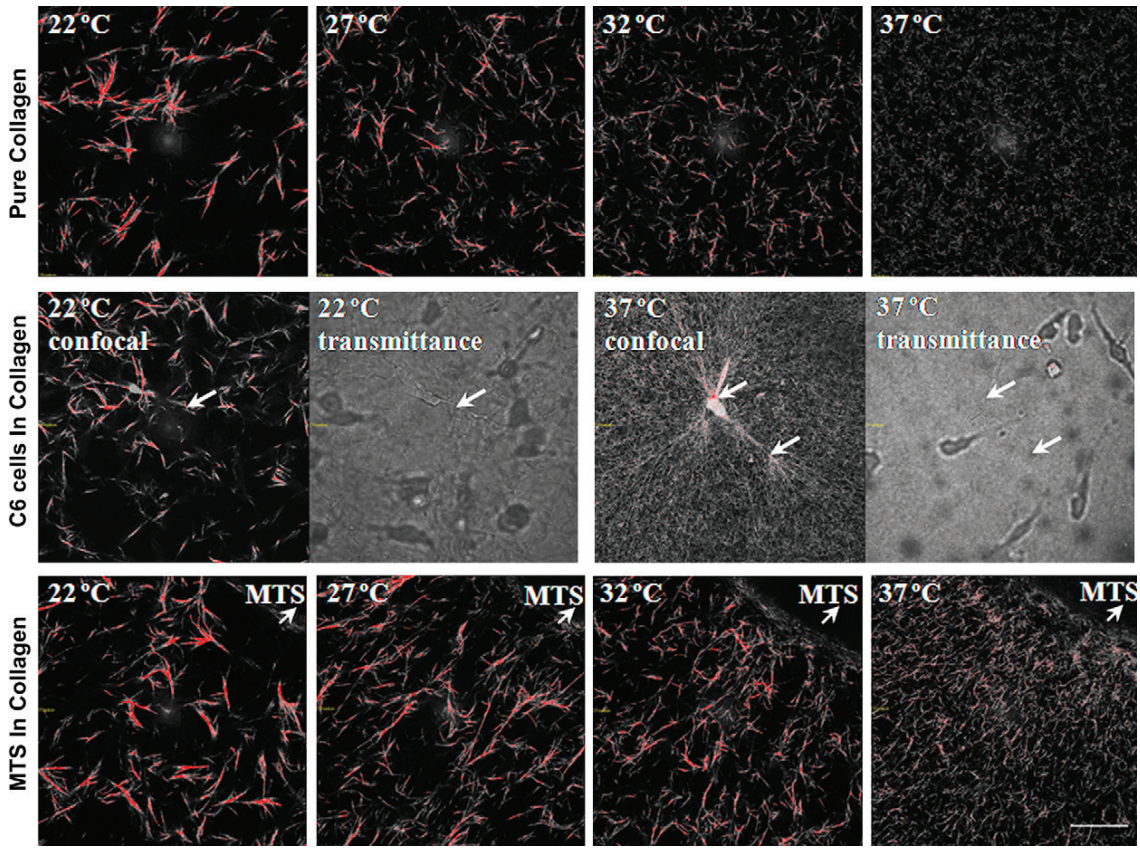

Fig. 4. 1.0 mg/ml collagen formed via the two-step two-temperature method. (first row) CRM of pure collagen nucleated at different temperatures from 22 to 37 °C. (second row) Confocal and transmittance images of cell-loaded collagen gels nucleated at 22 °C and 37 °C. Images were taken after 24 h of cell culture. Cells were embedded within the collagen gels. In focus cells are indicated by white arrows. (third row) CRM of MTS-loaded collagen nucleated at different temperatures. Images were taken near the MTS 2 h after implantation. White arrows indicate MTS position. Scale bar is 50 μm.

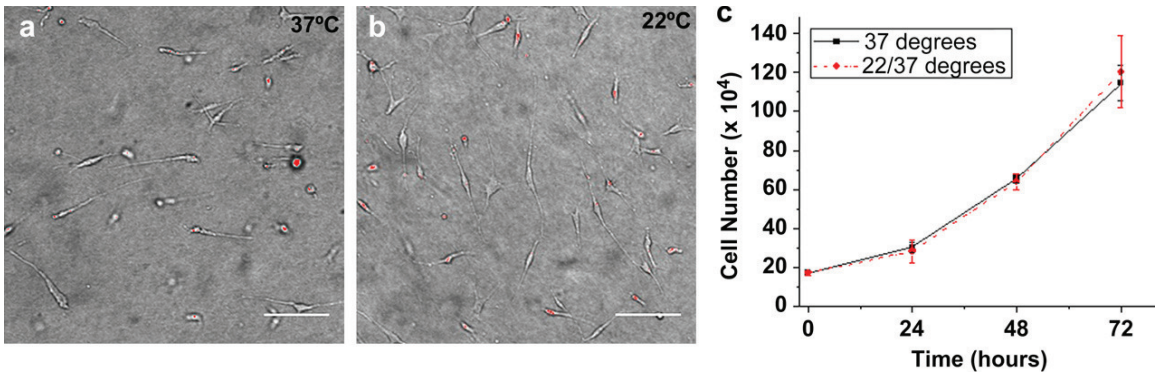

Fig. 5. Transmittance images of C6 cells embedded in 1.0 mg/ml collagen gels nucleated at (a) 37 °C and (b) 22 °C. Images were taken after 24 h of culture. Scale bar is 200 μm. (c) Number of live C6 cells averaged over 6 trials in gels either formed at 37 °C or nucleated at 22 °C over 72 h of culture.

somewhat earlier than arrest time, the structural measure of gelation reported by CRM [30]. Samples gelled initially at 22 °C for 2 min before the temperature was raised to 37 °C have stiffness very similar to gels formed entirely at 37 °C (Fig. 3). Samples gelled initially at 22 °C for 5 min before the temperature was raised to 37 °C have a modulus close to but slightly below those gelled at 22 °C (Fig. 3). Because the growth phase occurred over only ~3 min in these systems, it is difficult to quantify exactly how long the system must remain at 22 °C before attaining a stiffness characteristic of that of a system gelled entirely at 22 °C; however, our results strongly indicate the time associated with the lag phase of rheology is not sufficient but a time close to the arrest time is, in agreement with our imaging studies.

3.3. Cell-loaded gels formed by two-step gelation

The imaging and rheological experiments described above showed that the temperature dependent portion of 1.0 mg/ml collagen formed at temperatures as low as 22 °C was complete within 30 min. To confirm this, we gelled pure collagen (without cells) at 1.0 mg/ml at each of these temperatures for 30 min and then incubated at 37 °C for at least 1 h Fig. 4 confirms that fiber structure characteristic of each gelation temperature can be achieved by two-step gelation (Fig. 4, first row). As the nucleation temperature decreased from 37 to 22 °C, fibrils became increasingly bundled, fibrillar structures became thicker, and the pore size of the network increased for gels of the same concentration.

Cell-embedded collagen gels were then made by suspending cells in the collagen solutions at 4 °C and inducing collagen self-assembly in the presence of these cells by two-step gelation. Collagen-cell suspensions were nucleated at 22, 27, 32 °C for 30 min and then incubated at 37 °C. After 24 h of incubation at 37 °C following the initial 30 min incubation at lower temperature, cells in all gels appeared healthy and similar morphologically (Fig. 5a,b). To confirm non-cytotoxicity of this technique, live and total cell number were measured and found to be identical to within error for cells cultured in gels formed at 37 °C or first nucleated at 22 °C over 72 h (Fig. 5c). In both cases, cell viability was nearly 100%, and cell proliferation rate was unaffected by nucleation at 22 °C. C6-GFP cells embedded in 3D collagen fiber networks are shown in Fig. 4 (second row). Dual CFM and CRM images show cells and collagen fibers in the plane of the imaged cell(s) while transmitted light images show both the cells imaged with CFM (white arrows) and those outside the image plane. The cell imaged with CFM in the 22 °C nucleated gel is surrounded by sparse, thick fibers with no obvious alignment, while those in the 37 °C incubated gel are surrounded by a dense array of thin fibers that have been reorganized and aligned by the cells.

3.4. MTS invasion

To study glioma invasion in 3D, we worked with multicellular tumor spheroids (MTSs). Embedding such 3D tumor approximations in 3D gels allows for straightforward study of invasion, as several gradients that encourage invasion naturally occur in these systems. As in the dispersed cell experiments, spheroids were embedded in collagen solutions before gelation, and two-step two-temperature gelation was applied to create environments of different pore size but identical collagen concentration. Specifically, spheroid-embedded collagen gels of 1.0 mg/ml were gelled at 22, 27, and 32 °C for 30 min and then transferred to 37 °C to complete the gelation process. Collagen structures surrounding the spheroids 2 h after implantation are shown (Fig. 4, third row). Fibrillar structures characteristic of each nucleation temperature were observed, from thin fibrils at 37 °C to thick, bundled structures for gels nucleated at 22 °C. Structures surrounding the MTS tended to be aligned in a starburst pattern around the MTS, a pattern that has previously been shown to be a result of cell traction on these structures [37,38]. This alignment was consistently seen in gels nucleated at 37, 32 and 27 °C but was not always present in gels nucleated at 22 °C. This finding is consistent with the lack of reorganization of fibers around the dispersed cells in gels nucleated at 22 °C shown in Fig. 4 (middle row). Both results suggest that cells are less likely to reorganize a network with thick collagen bundles and large pores than one with thin fibrils and smaller pore size.

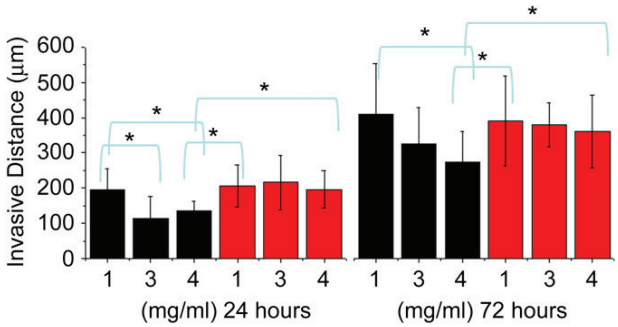

Fig. 6. MTS invasive distance at 24 and 72 h. MTSs were embedded in collagen of 1.0, 3.0 and 4.0 mg/ml gelled at 37 °C (black bars) or nucleated at 22 °C (red bars). Measurements were averaged over at least 5 MTSs. Asterisks show statistically significant results as assessed by two-tailed unpaired *t*-tests, with p values <0.05.

MTS invasion in 1.0 mg/ml collagen nucleated at different temperatures was monitored for 3 days. The invasive behavior over 72 h was found to be qualitatively similar in these gels, with fast migration over the first 24 h and somewhat slower migration over the next 48 h. For the 1.0 mg/ml gels, invasive distance (ID) at 72 h was similar for all four nucleation temperatures studied, with ID = 411 ± 144 μm at 37 °C and ID = 391 ± 127 μm at 22 °C (Fig. 6). While ID was very similar, the migratory pattern and morphology of the cells did differ somewhat between those embedded in 1.0 mg/ml gels constructed at 37 °C and those nucleated at 22 °C (Fig. 7a and b). In the 37 °C nucleated gel, invasion followed obvious paths in a starburst pattern, echoing the organization of collagen fibrils evident around the MTS in Fig. 4. At 37 °C, higher magnification imaging showed long, spindle-shaped cells near the invasion front parallel with aligned collagen fibers (Fig. 7c). In the 22 °C nucleated 1.0 mg/ml gels, particular paths of invasion were less obvious, and the invasive front was densely populated with cells that were less extended than those in the gel formed at 37 °C (Fig. 7d). Cells furthest from the spheroid center in the 1.0 mg/ml gel formed at 22 °C were also more rounded in general than were those in the 37 °C gel. The fact that cells were less elongated in the 22 °C nucleated gel may be related to the increased pore size, increased structural diameter, or other factors, as will be discussed further below.

To extend the range of pore sizes investigated, MTS invasion in 3.0 and 4.0 mg/ml collagen gels gelled at 37 °C or nucleated at 22 °C was monitored. As opposed to invasion in 1.0 mg/ml collagen gels, here spheroid invasion was significantly less successful in the 37 °C gel than in the 22 °C nucleated gel. Indeed, for spheroids allowed to invade for 72 h in collagen gels, statistically significant differences in ID were found between spheroids (1) in 4.0 mg/ml gels formed at 37 °C or nucleated at 22 °C, (2) in 1.0 and 4.0 mg/ml collagen gels formed at 37 °C, and (3) in 4.0 mg/ml gels formed at 37 °C and 1.0 mg/ml gels nucleated at 22 °C (Fig. 6). At 24 h following implantation, there was also a statistically significant difference in ID between spheroids in 1.0 and 3.0 mg/ml gels constructed at 37 °C. The more obvious differences in ID after 24 h relative to after 72 h is likely related to the fact that glioma cells may remodel their local environments through both traction generation and the use of matrix metalloproteases, constructing permissive paths to invasion over time and mitigating differences between environments that may otherwise affect invasive speed and patterns.

A key difference between the 4.0 mg/ml gel constructed at 37 °C and gels in which ID was significantly greater is that mesh size in the 4.0 mg/ml gel formed at 37 °C was the smallest of all the gels investigated. Here, mesh size was 2.3 ± 0.6 μm as measured near the MTS 2 h after spheroid implantation. This size is significantly smaller than typical glioma nuclear size, and such small pore size could be expected to impede migration via steric obstacles, as has been suggested by simulation and experiment on glioma cells previously [28,39,40]. Fig. 7 shows that the typical spheroid invasion pattern in 4.0 mg/ml collagen nucleated at 37 °C was similar to that observed for the 1.0 mg/ml gel formed at this temperature, though invasive distance was clearly decreased in the higher concentration gel. As in the 1.0 mg/ml gel, motile cells were elongated and arranged in a distinct starburst pattern.

While our approach allows for alteration of pore size independent of collagen concentration, several other structural and/or mechanical properties of the resulting network change alongside pore size, including structural diameter and bulk stiffness. These properties may each affect invasive distance as well as cell morphology and migratory phenotype. To investigate possible correlations between invasive distance and each of these variables, we plotted ID 24 h after MTS implantation in 1.0 and 4.0 mg/ml collagen gels nucleated at 22 °C or 37 °C as a function of pore size, stiffness, and average structural diameter of the gels (Fig. 8). Mesh size (Fig. 8a) was measured from collagen around the MTSs 2 h after implantation and was similar to measurements in cell-free conditions reported here (Figs. 1b and 2) and previously [21]. Pore size of gels constructed at 22 °C around the spheroids was somewhat smaller on average than those measured from gels nucleated at 22 °C in the absence of cells. This may be due to the early activity of spheroids in the gels as they generate traction on collagen fibers and begin to remodel their environment [38]. Stiffness of the gels was estimated from measurements in cell-free gels formed at 1.0 and 4.0 mg/ml at 37 °C or 22 °C (Fig. 8b). We note that batch to batch differences in acid-solubilized collagen lead to somewhat less bundling for low temperature gelation than seen in our previous study: as such, for gelation at low temperature, pore size was somewhat smaller and stiffness somewhat lower than that found in the previous study [21]. Gels constructed at 37 °C, however, were very similar in stiffness and pore size to those described previously and thus we estimated average fibril diameter in these gels from SEM measurements we reported previously [21]. To estimate average structural diameter in the gels nucleated at 22 °C, we used the relationship $G' \sim \xi^{-4.4} d^{5.6}$, with ξ measured mesh size, G' measured stiffness, and d an average structural diameter averaged over individual fibrils and fibril bundles as described in Section 2.8. Given the coupling of stiffness, structural diameter, and mesh size, it is not possible to fully decouple the effects of these parameters on glioma invasion in collagen gels. However, comparing gels of very similar pore size but different collagen content, stiffness, and structural diameter, for example, allows insight into the relative importance of pore size compared to the other variables in determining invasive behavior. Fig. 8 reveals some correlation between ID and both pore size and structural diameter of gels investigated here, though no correlation with bulk gel stiffness. Over the pore size range investigated, there was a monotonic increase of ID with pore size, though relatively little difference in ID with gels exhibiting pore size in the range of 5–12 μm. Similarly, there was a modest correlation between ID and structural diameter. No correlation was apparent between ID and bulk gel stiffness even though this was the only variable investigated that spanned more than one order of magnitude. Instead, here we found minimum ID in a relatively stiff gel but found another even stiffer gel supported more significant invasion. We argue this was due to the significantly different pore size in these two stiff gels, with the one with larger pore size supportive of invasion despite its bulk stiffness. Indeed, we note that in the two types of gels with most similar pore size (1.0 mg/ml collagen gelled at 37 °C and 4.0 mg/ml collagen nucleated at 22 °C), ID was nearly identical even though the stiffness of these gels differed by an order of magnitude and their average structural diameter was also quite dissimilar.

Despite the fact that ID and pore size appeared to correlate quite strongly in the gels investigated in this study, invasive distance is only one measure of invasive behavior of such cells. Imaging of cells in the 1.0 mg/ml gel formed at 37 °C and the 4.0 mg/ml collagen nucleated at 22 °C did reveal differences despite their similar invasive success as judged by ID. The morphology of cells in 4.0 mg/ml gels was less extended and aligned than in 1.0 mg/ml gels formed at 37 °C (Fig. 7h vs. c). However, these cells were also significantly more extended than those in the 1.0 mg/ml gel formed at 22 °C (Fig. 7d), where many cells were rounded. These findings suggest that a property other than pore size contributes to the detailed invasive cell morphology. To further investigate how fully pore size sets glioma invasive behavior, time-lapse microscopy was performed during spheroid invasion in gels with similar mesh size: 1.0 mg/ml collagen nucleated at 37 °C and 4.0 mg/ml collagen nucleated at 22 °C, as well as in 1.0 mg/ml collagen nucleated at 22 °C. Most invading cells in 1.0 mg/ml collagen nucleated at 37 °C

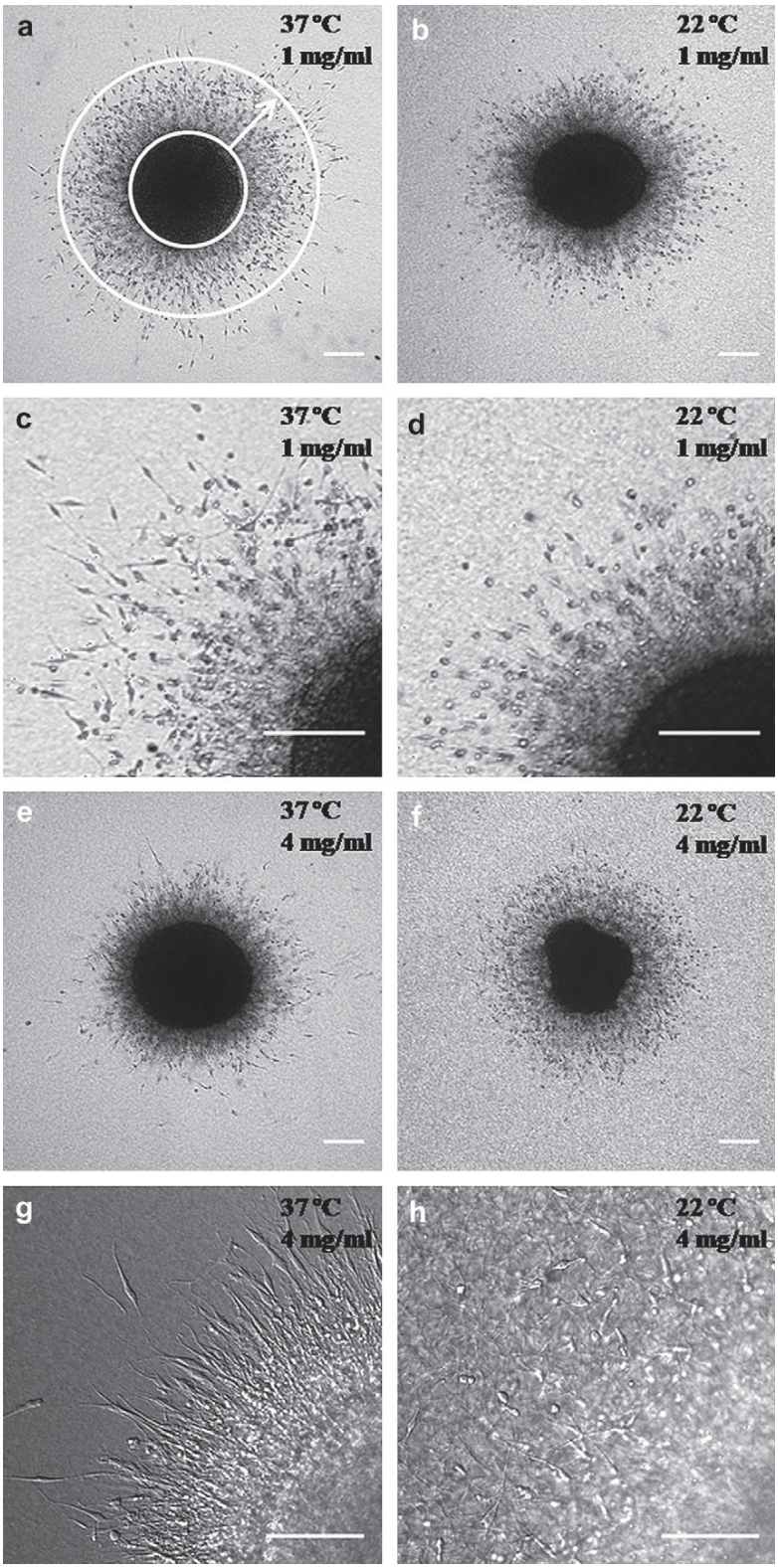

Fig. 7. MTS invasion in 1.0 and 4.0 mg/ml collagen gels nucleated at 37 °C or 22 °C. (a), (b), (e) and (f) show invasion patterns and (c), (d), (g) and (h) show higher magnification images revealing morphology of invading cells. All images were taken 3 days after implantation. Invasive distance is depicted by the arrow shown in (a), by assessing distance between the dense portion of the spheroid and the average extent of invasive cells. (a)–(f) are transmittance images, while (g) and (h) are DIC images that enhance contrast between cells and the surrounding fibers. Scale bar is 200 μm.

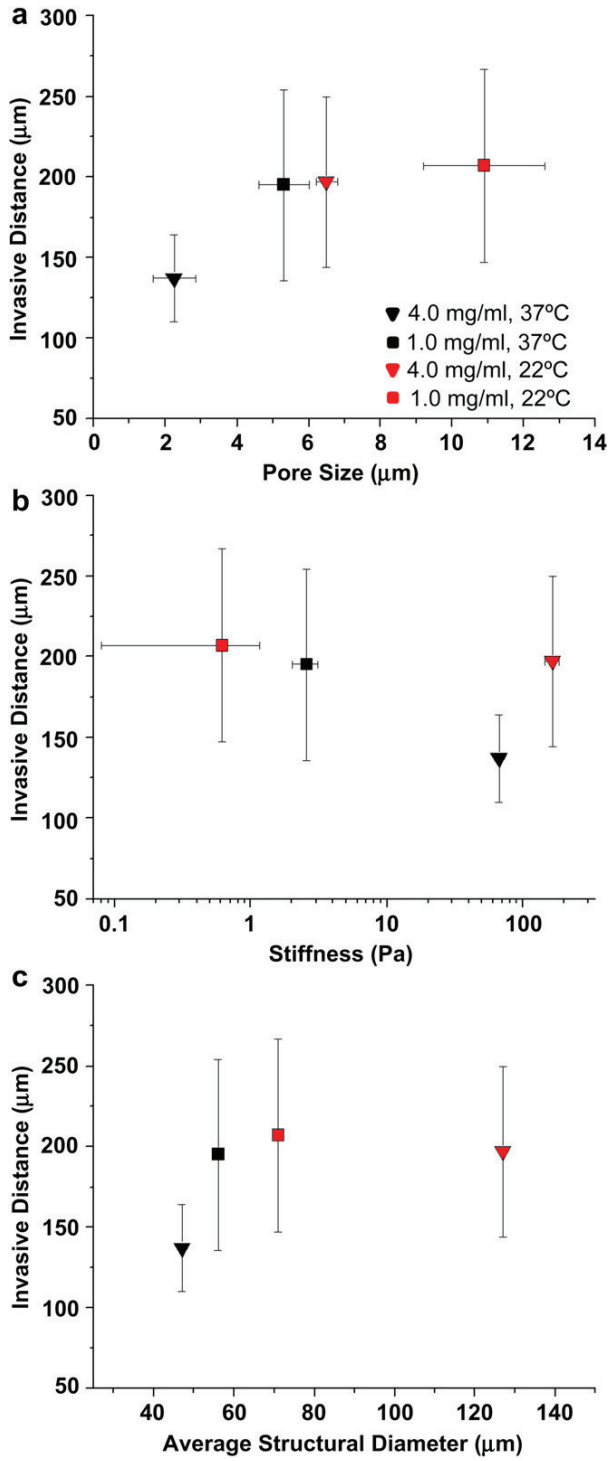

Fig. 8. MTS invasive distances 24 h after implantation are plotted as a function of (a) pore size, (b) stiffness (storage modulus, G′) and (c) average structural diameter. MTSs were embedded in collagen of 1.0 mg/ml (squares) or 4.0 mg/ml (triangles) nucleated at 22 °C (red) or 37 °C (black). Pore size was determined from measurements around at least 5 MTSs 2 h after implantation and is similar to mesh size measured in gels of the same concentration and at the same temperature in the absence of cells. Stiffness was measured via rheology on gels prepared in the absence of cells. Structural diameter was calculated as described in the text.

had the morphology and invasive behavior seen in glioma cells in mouse models [28]. The detached cells had a long leading filopodium and a short trailing edge. During invasion, the leading edge of the cell extended continuously, while the cell body moved in a saltatory fashion. Sometimes these cells underwent hourglass-like deformations of the nucleus during migration through small pores. Invading cells in collagen nucleated at 22 °C had different morphologies: some were spindle-shaped and extended while others were more spherical. During invasion, the more spherical cells exhibited flexible shape changes reminiscent of amoeboid morphology [41], while extended cells moved more similarly to those in the 1.0 mg/ml 37 °C gel, perhaps reflective of differences in local collagen environments around particular cells. Additionally, much less collagen remodeling was seen in the 22 °C gels than in the 1.0 mg/ml 37 °C collagen gels, consistent with images in Fig. 4. The amoeboid motility seen for some cells in the 22 °C environments may be related to cell inability to reorganize and/or dissolve the thicker surrounding structures sufficiently to effect mesenchymal motility [13,41].

4. Discussion

Through microscopy and rheology studies, we have confirmed that the first portion of collagen gelation is temperature dependent, and this initial temperature sets both overall network structure (pore size) in the gel and structural diameter of the fibrils and/or fibers that compose the network. The temperature dependent portion of gelation is similar to arrest time as measured by CRM, a time at which the structure of the gel includes a relatively small proportion of the structures present in the equilibrium network. Additionally, we have shown that the temperature dependent portion of gelation encompasses both the lag phase and a portion of the growth phase as judged by the development of the storage modulus in rheological tests. We note that this temperature dependent portion of gelation extends beyond nucleation as traditionally defined in which only very small aggregates are present; here, no or very few fibers would be apparent in CRM and a very small storage modulus would be evident in rheology. Despite this difference, the overall finding of a temperature dependent and independent phase of collagen gelation is consistent with that proposed by Wood [22].

The presence of a relatively short temperature dependent stage of gelation allows for preparation of collagen environments of identical concentration but different pore size (or vice-versa) in the presence of cells in a manner that minimizes potential convolution of effects of different cell culture conditions with that of different properties of the collagen environment. For the acid-solubilized collagen employed here, the temperature dependent portion of gelation was found to be less than 30 min at the lowest temperature investigated (22 °C), which allows nucleation to be performed in the presence of cells without impacting cell viability. This approach would not be useful for all collagen I based ECM approximations: indeed, pepsin-solubilized collagen undergoes much slower gelation due to lack of telopeptides [23,31–34]. We found previously that 1.0 mg/ml pepsin-solubilized collagen takes 10–15 min to attain its equilibrium storage modulus for gelation at 37 °C and nearly an hour to do so at 32 °C, while for the acid-solubilized collagen investigated here, this occurs within 5 min at 37 °C and 32 °C [30]. Despite this key difference, we propose that the nucleation and growth mechanism of collagen gelation can be exploited to make cell-embedded, pore size variable pepsin-solubilized gels as well. Here, we suggest adding cells after the temperature dependent portion of gelation; since few fibers are present at this point, addition of cells should be possible without significant network perturbation.

We have performed two-step two-temperature gelation to create environments of different pore size at identical concentration (and vice-versa) in the absence of cells, presence of dispersed glioma cells, and presence of glioma spheroids. Cell viability was not affected by 30 min gelation at any of the temperatures investigated. For spheroid invasion studies, we found that invasive distance was very similar for gels of identical pore size even when these gels were of different collagen concentration, gelation temperature, bulk stiffness, and local stiffness as set by structural diameter. This finding suggests that a driving force for glioma invasion in these gels is the presence of ligands onto which integrins can adhere and generate traction. In 2D spreading and migration experiments, it has been shown that an intermediate density of such ligands optimizes cell migration [8,42]. While we have not investigated very large pore size networks here, where it would be expected that insufficient tethers on which to generate traction would limit migration [37], we did find that migration is hindered by small pore size and that invasive distance was not very sensitive in the range of pore size from ~5 to 12 μm. At small pore size, a variety of factors, including high ligand density that does not encourage the cell polarity and release seen in mesenchymal migration likely contributes to the limited invasion [40]. For environments with pore size in the optimal range, we found similar success as measured by invasive distance and invasive cell density *even when the gels have markedly different bulk and local stiffness*, which is influenced most strongly by thickness of the struts of the network for gels of identical pore size. Biochemically, differences in structural thickness likely do not affect the number of ligands available for cell adhesion even when the overall collagen concentrations of the systems differ. For these reasons, we believe that pore size and ligand density in collagen gels are key factors in setting invasive speed of glioma cells in such environments and are more important than either bulk or local stiffness. More subtle measures of invasive behavior than invasive distance are clearly not fully set by pore size of the network: indeed, the presence of a population of extended cells that move in a saltatory manner together with a population of non-extended cells that move in a more amoeboid fashion in gels of 1.0 and 4.0 mg/ml nucleated at 22 °C suggests that local thickness of the fibers adjacent to a particular cell and thus local stiffness of the environment may set migratory phenotype. Additional investigation of local glioma cell–collagen interactions can yield additional insight on how such properties affect cell invasive behavior.

5. Conclusions

In this work, gelation temperatures from 22 to 37 °C were used to control the pore size of cell-loaded collagen matrices independent of collagen concentration. To limit cell exposure to temperatures below physiological temperature, we investigated the time required to establish fiber and network structure in these gels with CRM and rheology. We conclude that the temperature dependent portion of collagen gelation ends at a time similar to the arrest time as measured by CRM and in the growth phase as measured by rheology. We exploited these findings to create cell-embedded collagen nucleated at 22, 27, and 32 °C for 30 min and then incubated at 37 °C for the remainder of self-assembly. This achieved fibrillar and network structure characteristic of gels constructed entirely at the nucleation temperature. Glioma invasion in these gels suggests that moderate pore size, independent of global collagen concentration and both local and bulk stiffness, is a key factor in setting invasive speed of glioma cells, though not all aspects of invasive cell phenotype.

Acknowledgments

This work was funded in part through a Beckman Young Investigator Award.

Appendix

Figures with essential colour discrimination. Figs. 1-6 and 8 in this article are difficult to interpret in black and white. The full colour images can be found in the on-line version, at doi:10.1016/j.biomaterials.2010.03.039.

References

[1] Alberts B, Johnson A, Lewis J, Raff M, Roberts K, Walter P. Molecular biology of the cell. New York: Garland Science; 2002.
[2] Comper WD. Extracellular matrix. Amsterdam: Harwood Academic Publishers; 1996.
[3] Pedersen JA, Swartz MA. Mechanobiology in the third dimension. Ann Biomed Eng 2005;33:1469–90.
[4] Kuntz RM, Saltzman WM. Neutrophil motility in extracellular matrix gels: mesh size and adhesion affect speed of migration. Biophys J 1997;72:1472–80.
[5] Lo CM, Wang HB, Dembo M, Wang YL. Cell movement is guided by the rigidity of the substrate. Biophys J 2000;79:144–52.
[6] Bischofs IB, Schwarz US. Cell organization in soft media due to active mechanosensing. Proc Natl Acad Sci U S A 2003;100:9274–9.
[7] Grinnell F. Fibroblast biology in three-dimensional collagen matrices. Trends Cell Biol 2003;13:264–9.
[8] Gaudet C, Marganski WA, Kim S, Brown CT, Gunderia V, Dembo M, et al. Influence of type I collagen surface density on fibroblast spreading, motility, and contractility. Biophys J 2003;85:3329–35.
[9] Discher DE, Janmey P, Wang YL. Tissue cells feel and respond to the stiffness of their substrate. Science 2005;310:1139–43.
[10] O'Brien FJ, Harley BA, Yannas IV, Gibson LJ. The effect of pore size on cell adhesion in collagen–GAG scaffolds. Biomaterials 2005;26:433–41.
[11] Engler AJ, Sen S, Sweeney HL, Discher DE. Matrix elasticity directs stem cell lineage specification. Cell 2006;126:677–89.
[12] Zaman MH, Trapani LM, Siemeski A, MacKellar D, Gong HY, Kamm RD, et al. Migration of tumor cells in 3D matrices is governed by matrix stiffness along with cell–matrix adhesion and proteolysis. Proc Natl Acad Sci U S A 2006;103:10889–94.
[13] Friedl P, Brocker EB. The biology of cell locomotion within three-dimensional extracellular matrix. Cell Mol Life Sci 2000;57:41–64.
[14] Wood GC, Keech MK. The formation of fibrils from collagen solutions. 1. The effect of experimental conditions: kinetic and electron-microscope studies. Biochem J 1960;75:588–98.
[15] Williams BR, Gelman RA, Poppke DC, Piez KA. Collagen fibril formation. Optimal in vitro conditions and preliminary kinetic results. J Biol Chem 1978;253:6578–85.
[16] Christiansen DL, Huang EK, Silver FH. Assembly of type I collagen: fusion of fibril subunits and the influence of fibril diameter on mechanical properties. Matrix Biol 2000;19:409–20.
[17] Roeder BA, Kokini K, Sturgis JE, Robinson JP, Voytik–Harbin SL. Tensile mechanical properties of three-dimensional type I collagen extracellular matrices with varied microstructure. J Biomech Eng 2002;124:214–22.
[18] Liu MY, Yeh ML, Luo ZP. In vitro regulation of single collagen fibril length by buffer compositions and temperature. Biomed Mater Eng 2005;15:413–20.
[19] Raub CB, Suresh V, Krasieva T, Lyubovitsky J, Mih JD, Putnam AJ, et al. Noninvasive assessment of collagen gel microstructure and mechanics using multiphoton microscopy. Biophys J 2007;92:2212–22.
[20] Raub CB, Unruh J, Suresh V, Krasieva T, Lindmo T, Gratton E, et al. Image correlation spectroscopy of multiphoton images correlates with collagen mechanical properties. Biophys J 2008;94:2361–73.
[21] Yang YL, Leone LM, Kaufman LJ. Elastic moduli of collagen gels can be predicted from two dimensional confocal microscopy. Biophys J 2009;97:2051–60.
[22] Wood GC. The formation of fibrils from collagen solutions. 2. A mechanism of collagen-fibril formation. Biochem J 1960;75:598–605.
[23] Comper WD, Veis A. The mechanism of nucleation for in vitro collagen fibril formation. Biopolymers 1977;16:2113–31.
[24] Giese A, Bjerkvig R, Berens ME, Westphal M. Cost of migration: invasion of malignant gliomas and implications for treatment. J Clin Oncol 2003;21:1624–36.
[25] Lefranc F, Brotchi J, Kiss R. Possible future issues in the treatment of glioblastomas: special emphasis on cell migration and the resistance of migrating glioblastoma cells to apoptosis. J Clin Oncol 2005;23:2411–22.
[26] Thorne RG, Nicholson C. In vivo diffusion analysis with quantum dots and dextrans predicts the width of brain extracellular space. Proc Natl Acad Sci U S A 2006;103:5567–72.

[27] Soroceanu L, Manning TJ, Sontheimer H. Modulation of glioma cell migration and invasion using Cl^- and K^+ ion channel blockers. J Neurosci 1999;19:5942–54.
[28] Beadle C, Assanah MC, Monzo P, Vallee R, Rosenfeld SS, Canoll P. The role of myosin II in glioma invasion of the brain. Mol Biol Cell 2008;19:3357–68.
[29] Mackintosh FC, Kas J, Janmey PA. Elasticity of semiflexible biopolymer networks. Phys Rev Lett 1995;75:4425–8.
[30] Yang YL, Kaufman LJ. Rheology and confocal reflectance microscopy as probes of mechanical properties and structure during collagen and collagen/hyaluronan self-assembly. Biophys J 2009;96:1566–85.
[31] Comper WD, Veis A. Characterization of nuclei in in vitro collagen fibril formation. Biopolymers 1977;16:2133–42.
[32] Hayashi T, Nagai Y. Factors affecting interactions of collagen molecules as observed by in vitro fibril formation. 3. Non-helical regions of collagen molecules. J Biochem 1974;76:177–86.
[33] Capaldi MJ, Chapman JA. The C-terminal extra-helical peptide of type I collagen and its role in fibrillogenesis in vitro. Biopolymers 1982;21:2291–313.
[34] Kuznetsova N, Leikin S. Does the triple helical domain of type I collagen encode molecular recognition and fiber assembly while telopeptides serve as catalytic domains? Effect of proteolytic cleavage on fibrillogenesis and on collagen–collagen interaction in fibers. J Biol Chem 1999;274:36083–8.
[35] Forgacs G, Newman SA, Hinner B, Maier CW, Sackmann E. Assembly of collagen matrices as a phase transition revealed by structural and rheologic studies. Biophys J 2003;84:1272–80.
[36] Brightman AO, Rajwa BP, Sturgis JE, McCallister ME, Robinson JP, Voytik-Harbin SL. Time-lapse confocal reflection microscopy of collagen fibrillogenesis and extracellular matrix assembly in vitro. Biopolymers 2000;54:222–34.
[37] Kaufman LJ, Brangwynne CP, Kasza KE, Filippidi E, Gordon VD, Deisboeck TS, et al. Glioma expansion in collagen I matrices: analyzing collagen concentration-dependent growth and motility patterns. Biophys J 2005;89:635–50.
[38] An Z, Gluck CB, Choy ML, Kaufman LJ. Suberoylanilide hydroxamic acid limits migration and invasion of glioma cells in vitro. Cancer Lett 2010;292:215–27.
[39] Rubenstein BM, Kaufman LJ. The role of extracellular matrix in glioma invasion: a cellular Potts model approach. Biophys J 2008;95.
[40] Ulrich TA, Jain A, Tanner K, MacKay JL, Kumar S. Probing cellular mechanobiology in three-dimensional culture with collagen–agarose matrices. Biomaterials 2010;31:1875–84.
[41] Wolf K, Mazo I, Leung H, Engelke K, von Andrian UH, Deryugina EI, et al. Compensation mechanism in tumor cell migration: mesenchymal–amoeboid transition after blocking of pericellular proteolysis. J Cell Biol 2003;160:267–77.
[42] Palecek SP, Loftus JC, Ginsberg MH, Lauffenburger DA, Horwitz AF. Integrin-ligand binding properties govern cell migration speed through cell–substratum adhesiveness. Nature 1997;385:537–40.